SIMULATION AND OBSERVATION OF THE FRACTURE PROCESS ZONE

T. Steiger, H. Sadouki, and F.H. Wittmann,
Laboratory for Building Materials, Swiss Federal Institute of Technology
Zürich, Switzerland

Abstract
The determination of the extension of the fracture process zone in composite materials such as cement or polymer mortar is rather difficult. Non destructive techniques must be applied in order to observe the evolution of the deterioration of the material. Fracture tests carried out in an environmental scanning electron microscope allow us to observe the development of the fracture process zone and crack propagation under increasing load. The experimental results will be compared with results obtained by numerical simulation based on the fictitious crack model.

1 Introduction

Today the fictitious crack model (FCM) is widely used to predict crack formation in composite materials such as concrete. One basic assumption of this approach is the formation of a fictitious crack. It is assumed that within the fictitious crack depending on the the actual width, tensile forces can still be transmitted. So far few attempts exist to observe the existence of a fictitious crack in order to validate numerical predictions.

Knab (Knab et al. (1986)) has summarized some useful techniques which had been applied to observe the fracture process zone. Hu (1990,

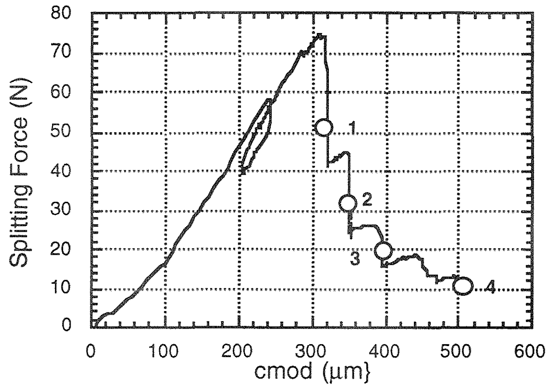

Fig. 2. Measured load-displacement curve of polymer mortar with points indicating the states at which micrographs of Fig. 4 have been taken

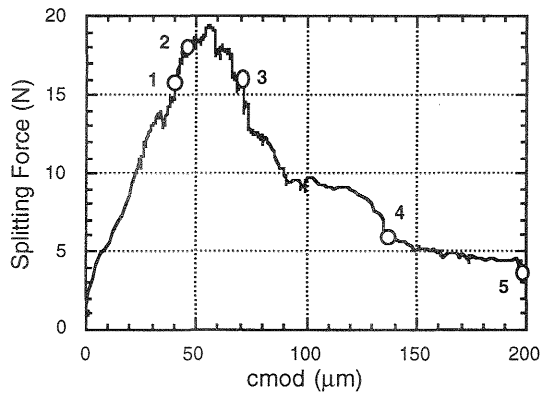

Fig. 3. Measured load-displacement curve of cement mortar with points indicating the states at which micrographs of Fig. 5 and Fig. 6 have been taken

3.2 Widening of the fictitious crack

To observe the widening of the fictitious crack in polymer mortar it was decided to follow the crack evolution at a point approximately 1.8mm apart from the notch tip. Immediately after the maximum in the force-displacement diagram had been passed a first photo is taken (Fig 2.1). A continuous crack can be observed. It is quite obvious that, per unit of length of the fictitious crack an average load can be transfered by the still existing bridges. A further stage of deterioration is marked with point 2 in Fig. 2. The corresponding opening is shown in Fig. 4.2. The micrographs shown in Fig. 4.3 and 4.4 correspond to the situation marked with 3 and 4 in Fig. 2

2.3 Preparation of specimens

We prepared mixes with two different types of binder: an epoxy resin hardener system and a portland cement. Crushed grains of a maximum size of 200µm were embedded in the cement and polymer mortar. For both mortars the volume concentration of aggregates was chosen to be 35%. This corresponds to the composition of fine mortar in concrete.

The specimens used to carry out in-situ experiments have been cast in standard moulds (160*160*40mm). With a diamond bladed saw the final geometry of the WOD-specimen (30*30*5mm) was cut. Using a special saw the notch was cut (notch width of 0.5mm). The ligament has a length of 10mm. In Fig. 1 the geometrical shape of the specimens is given.

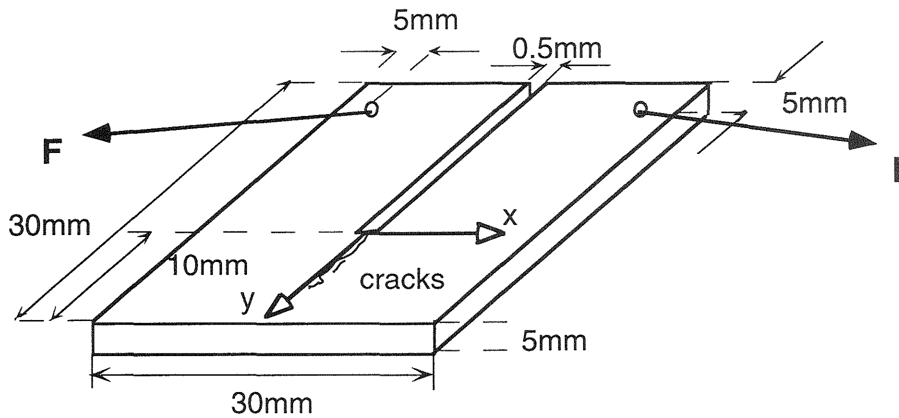

Fig. 1. Schematic representation of WOD-specimens for polymer and cement mortar

3 Experimental Results

3.1 Force-displacement diagrams

In Fig. 2 the force-displacement diagram of a polymer mortar as being tested under electron microscopical observation is shown. The indicated numbers point out the corresponding levels along the softening branch at which microphotos have been taken.

In Fig. 3 the equivalent force-displacement diagram as observed on cement mortar specimen is plotted. From these experimental results the fracture energy and the strain-softening relation have been determined by inverse analysis.

1993) has successfully applied the multi-cutting technique in order to determine the effective length of the fracture process zone. By optical interferometry Rastogi and Denarié (1994) have also observed the extension of the fracture process zone. A similar technique has been applied by Hack et al. (1995).

Mindess and Diamond (1980) and Diamond et al. (1983) were probably the first to observe crack formation directly in an electron microscope. In this way characteristic features along the crack path can be observed.

With the aim to observe mechanisms of load transfer and mechanisms of energy consumption in the fracture process zone and to quantitatively follow the evolution we carried out tests on polymer and cement mortar in an Environmental Scanning Electron Microscope (ESEM). We applied the load by a specially developed device which allows us to fracture specimens under wedge opening displacement (WOD). The experimental results should serve as a basis for comparison with results of numerical simulations. The numerical model used in this comparative study is based on the (FCM) according to Hillerborg et al. (1976).

2 Experimental set-up and preparation of specimen

2.1 Low vacuum scanning electron microscopy

The specimen chamber of the microscope is operated with a controlled environment (Danilatos and Robinson (1979)), while the optical column is kept under high vacuum. The relatively high gas pressure in the specimen chamber allows us to work without additional preparation of the surface (Ollivier (1985)). In this instrument non-conductive surfaces can be observed. During testing the specimen chamber was kept at about 1-2 Torr and about 25°C. The primary electrons were accelerated by 17keV in the case of the cement mortar specimens and 18 keV in the case of the polymer mortar specimens.

2.2 In-situ testing machine

Wedge splitting tests were run on a special in-situ testing machine mounted on a coordinate table in order to control the position of observation. The test device consists of a stiff frame to support the specimen and the loading wedge (wedge angle α=15°), a strain gauge and a load cell. Loading and unloading of the specimen is carried out by remote control. The position of the specimen is approximately kept constant due to a contrarotating system. The splitting force and the displacement were continuously recorded during testing.

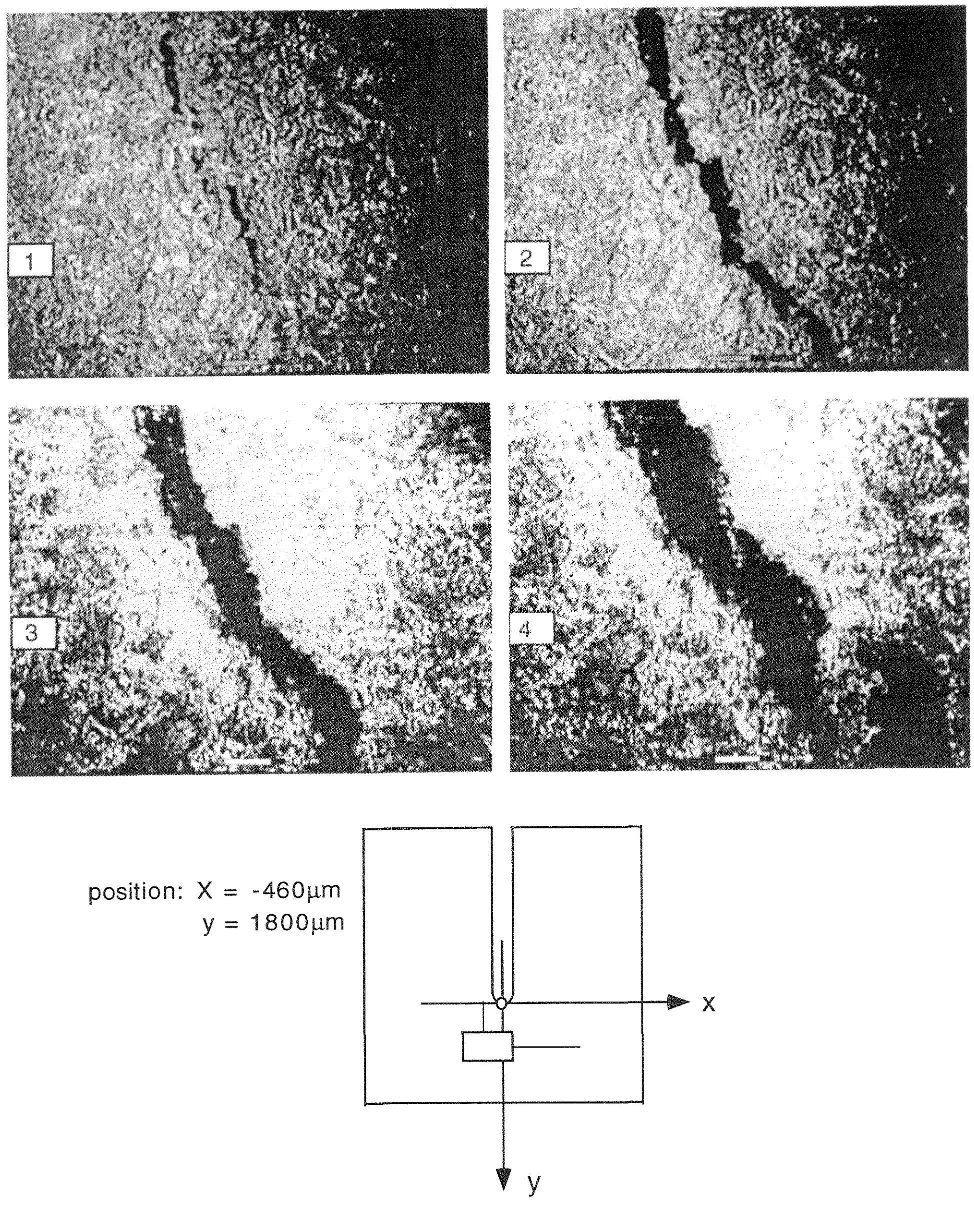

Fig. 4. Microphotos corresponding to load points 1 to 4 shown in the force-displacement diagram of Fig. 2

In Fig. 5 three different stages of crack formation in a cement mortar are shown. The corresponding points on the force-displacement diagram are marked with 1-3 in Fig. 3. In addition the crack width has been observed at a stage of higher damage (points 4 and 5). The place of observation and the micrographs are shown in Fig. 6.

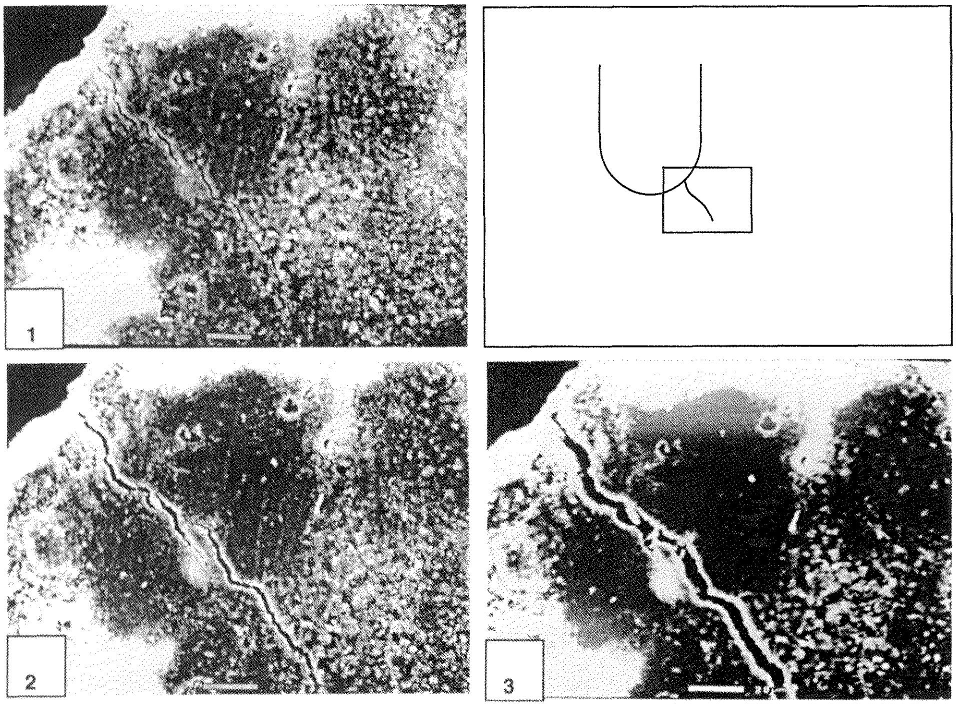

Fig. 5. Microphotos corresponding to load points 1 to 3 shown in the force-displacement diagram of Fig. 3

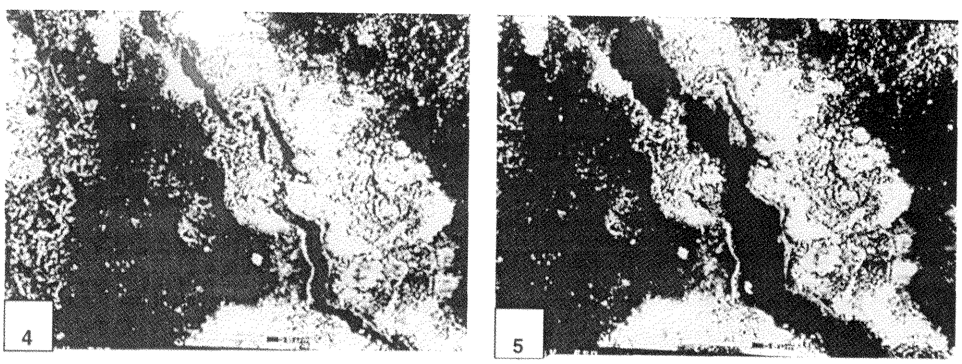

position: x = -80μm
y = 4010μm

Microphotos corresponding to load points 4 and 5 shown in the force-displacement diagram of Fig. 3

3.3 Determination of crack length

In order to be able to determine the length of both the real and the fictitious crack, microphotos have been taken along an existing crack path. A typical example is shown in Fig. 7. The crack tip can be clearly seen. The transition from real to fictitious crack is located where no bridges can been seen any more.

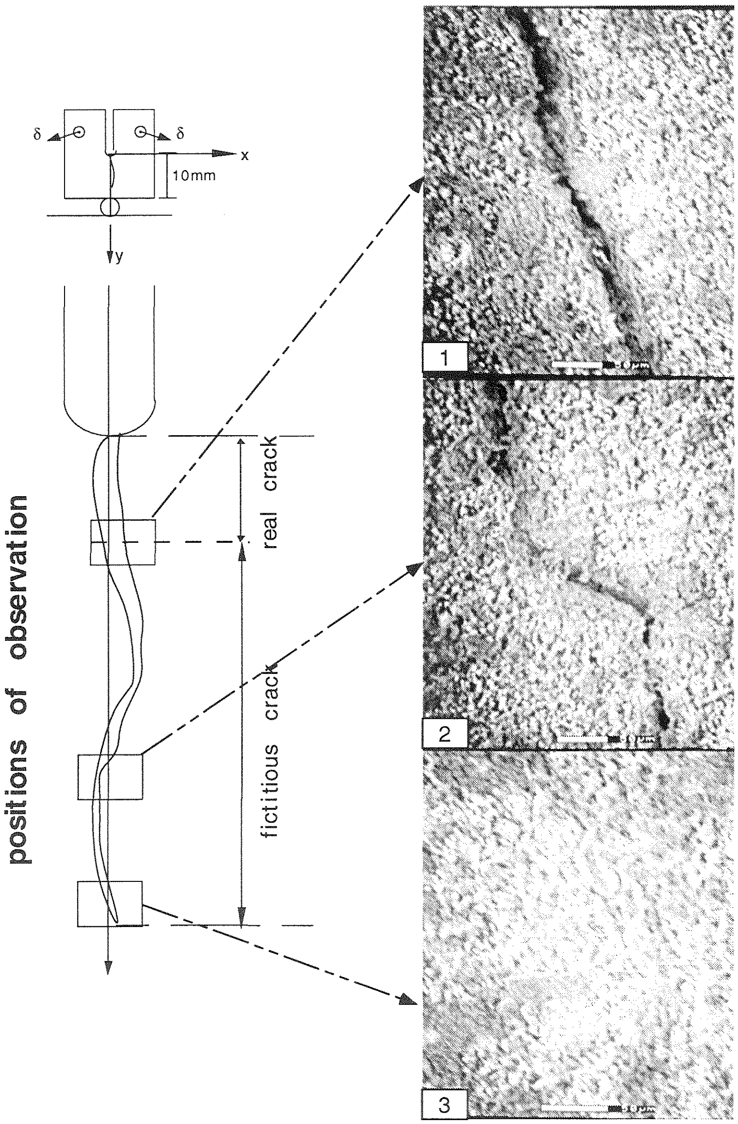

Fig. 7. Crack path with the transition from real to fictitious carck (1), an intermediate state (2) and the crack tip (3)

4 Numerical analysis and simulation

For the simulation of the formation of fictitious and real cracks we applied a cohesive crack model. The strain-softening behaviour is modelled by a bilinear curve defined by four material parameters (f_t, σ_1, w_1 and w_2). The area under the diagram is the fracture energy (G_f) given by the following equation:

$$G_f=0.5\,(f_t\,w_1+\sigma_1\,w_2) \tag{1}$$

In principle the strain-softening diagram can be directly obtained by uniaxial tension tests, but these tests are often difficult to be performed. For that reason, the softening diagram is derived from load-displacement diagrams obtained on WOD-specimens combined with an adequate inverse analysis (Roelfstra and Wittmann (1986)). Table 1 gives the relevant mechanical properties obtained for polymer and cement mortar.

Table 1. Fracture energy and strain-softening parameters

Material	E N/mm^2	G_f N/m	f_t MPa	σ_1 MPa	w_1 mm	w_2 mm
polymer mortar	5000	237	16.8	1.83	0.025	0.03
cement mortar	20000	34	4	1.4	0.01	0.02

In order to take the heterogenous character of the composite material into account we introduced a statistical distribution of the Young's modulus E and the tensile strength f_t.

The numerical analysis of crack formation of a WOD specimen was performed by means of the customary non-linear FE-package MARC (MARC 1994). Linking a special user subroutine 'TENSOF' the numerical treatment of the cracking process is possible. The mesh generation is carried out automatically taking the realistic boundary conditions into account.

In Fig. 8 and Fig.9 the strain-softening curves of polymer and cement mortar are shown. This result can be used for the comparison with experimental results.

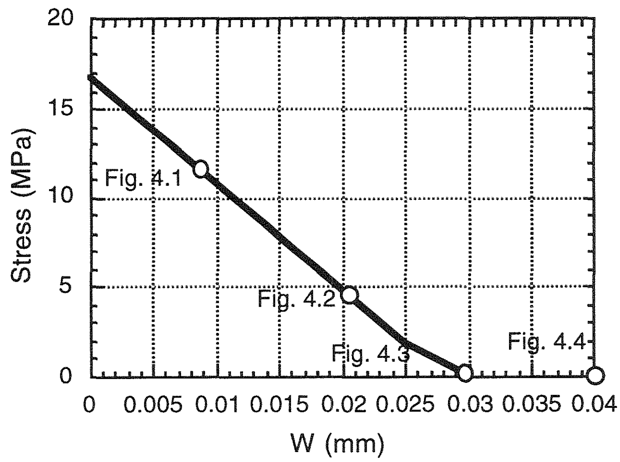

Fig. 8. Strain-softening of polymer mortar

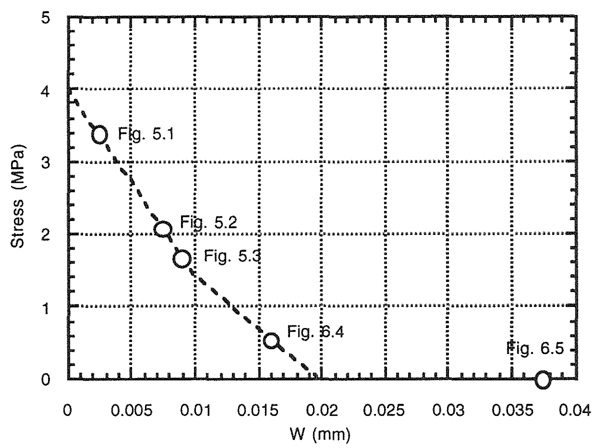

Fig. 9. Strain-softening of cement mortar

5 Comparison of experimental and numerical results and discussion

In Fig. 8 and Fig. 9 of the previous section the numerically determined strain-softening relations for polymer and cement mortar are shown. Along the descending branch the figures indicate the degree of damage which corresponds to the micrographs presented earlier. The points 4.1 and 4.2 for example correspond to the micrographs 1 and 2 shown in Fig. 4. In this way the degree of damage can be visualized.

The crack opening at a given point along the crack path has been calculated numerically by using the experimentally determined parameters. In Fig. 5 a typical example is shown. The crack opening (fictitious and real) as numerically predicted is compared with observations in the ESEM. A fair agreement is found, as it can be seen in Fig. 10. In Fig. 11, it is not the width but the length of the fictitious and the total (fictitious and real) crack which are shown. Again a reasonable agreement can be observed. It must be stated, however, that this comparison is not yet based on a statistical evaluation of many cracks. Therefore this contribution has to be considered as an attempt to develop a new method for the validation of numerical predictions.

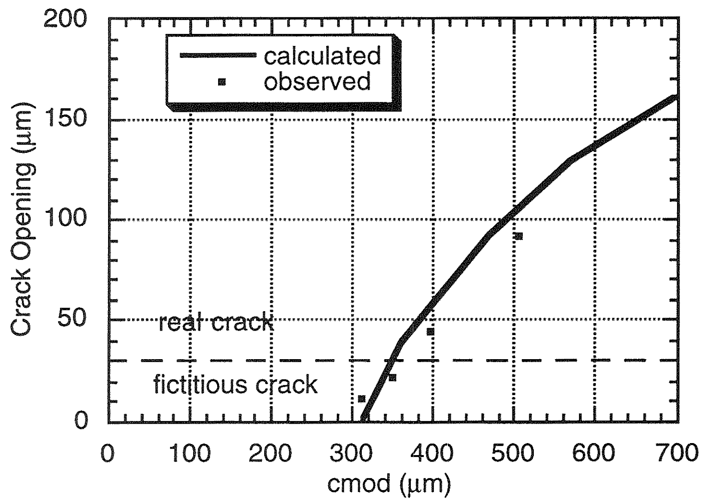

Fig. 10 Numerical and observed values of crack opening

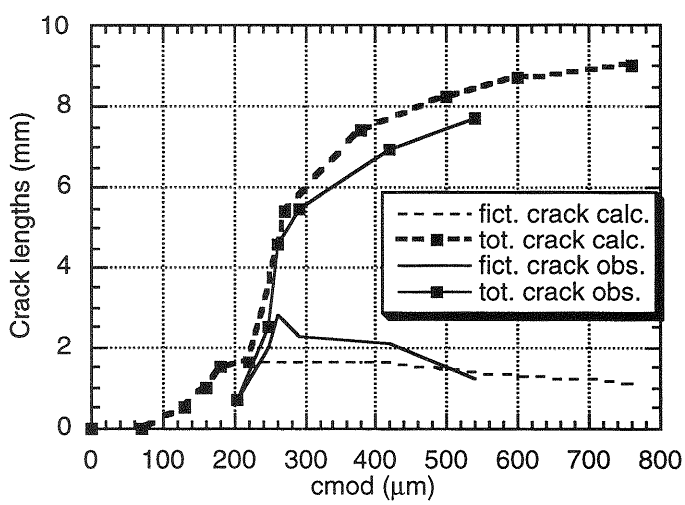

Fig. 11 Calculated and observed fictitious and total crack lengths

6. Conclusions

Basic assumptions of numerical models need to be experimentally verified. The extension, the width of the fictitious crack can be visualized by means of an electron microscopical observation. Results of a corresponding numerical simulation are in good agreement. This means that a numerical model based on the concept of the fictitious crack has a sound physical basis. The experimental results validate the main assumptions of the fictititous crack model.

The observation of the evolution of crack formation allows us to distinguish between different energy consuming mechanisms in the fictitious crack. Strain energy in remaining solid bridges, friction and interlocking all contribute to the energy consumption.

References

Danilatos, G.D, and Robinson V.N.E. (1979) Principles of scanning electron microscopy at high specimen chamber pressures, **Scanning**, 2:72-82

Diamond, S., Mindess, S, and Lovell, J. (1983) Use of a Robinson backscatter detector and "wet cell" for examination of wet cement paste and mortar specimens under load. **Cem. & Concr. Res.**, 13, 107-113

Hack, E., Steiger, T., and Sadouki, H. (1995) Application of electronic speckle pattern interferometry (ESPI) to oserve the fracture process zone, contribution to this volume.

Hillerborg, A., Modéer, M. and Petersson, P.E. (1976) Analysis of crack formation and crack growth in concrete by means of fracture mechanics and finite elements. **Cem. & Concr. Res.**, 6, 773-782.

Hu, X. (1990) Fracture process zone and strain-softening in cementitious materials, in **Building Materials Reports**, 1, AEDIFICATIO Publishers, Freiburg, Germany

Hu, X., and Wittmann, F.H. (1993) Characterisation of the fictitious crack with compliance measurements, in **Numerical Models in Fracture Mechanics of Concrete**, (ed. F.H. Wittmann), A.A. Balkema, Rotterdam, Brookfield.

Knab, L.I., Jennings, H., Walker, H.N., Clifton, J.R., and Grimes, J.W. (1986) Techniques to observe the fracture zone in mortar and concrete, in: **Fracture Toughness and Fracture Energy of Concrete** (ed. F.H. Wittmann), Elsevier,Amsterdam.

MARC Research Libary, Vol. C : Program Input. Marc Analysis Research Coorparation, Palo Alto (U.S.A.), 1994.

Mindess, S. and Diamond, S. (1980) A preliminary SEM study of crack propagation in mortar. **Cem. & Concr. Res.**, 10, 509-519

Ollivier, J.P. A non destructive procedure to observe the microcracks of concrete by scanning electron microscopy. **Cem. & Concr. Res.**,15, 1055-1060

Roelfstra, P.E. and Wittmann, F.H. (1986) Numerical Method to link strain softening with failure of concrete, in **Fracture Toughness and Fracture Energy of Concrete** (ed. F.H. Wittmann), Elsevier, Amsterdam.